ELSEVIER

Thin Solid Films 284–285 (1996) 836–840

thin solid films

Refractive index and layer thickness of an adsorbing protein as reporters of monolayer formation

R.G.C. Oudshoorn, R.P.H. Kooyman *, J. Greve

Bio-Interface Group, MESA Institute, Department of Applied Physics, University of Twente, P.O. Box 217, 7500 AE Enschede, The Netherlands

Abstract

A method is presented for a separate real-time determination of refractive index and layer thickness of an adsorbing thin layer. The changing angular deflections of TE and TM modes in a dedicated planar waveguide structure are measured. A resolution of 0.01 in the refractive index and 0.5 nm in the average thickness is obtained. The method is illustrated with experimental results on the binding of an antibody to the substrate, both in a physisorption and in an immunoreaction. In the latter, results are consistent with an end-on binding of the antibody to the surface.

Keywords: Optical waveguide; Protein adsorption; Monolayers; Evanescent field

1. Introduction

Several experimental methods have been applied in the study of protein-covered surfaces. Particularly optical methods are useful in view of their high intrinsic sensitivity and relatively simple instrumentation, that allows for studying surfaces in a water environment. However, it has not yet been feasible to determine surface orientations and/or conformations using vibrational spectroscopy. Other optical methods that measure the overall dielectric properties of the protein, such as ellipsometry [1,2] and SPR [3,4] are very sensitive to the "optical thickness" of the layer under study, and sub-monolayer quantities can easily be quantified.

However, this "optical thickness" is a composite parameter including both the layer thickness and refractive index of the layer. Obviously, it would be much more informative if the optical thickness could be resolved in these two parameters, because one then has some additional knowledge about the packing density of the adsorbed molecules, which, at least in principle, can be interpreted in terms of molecular conformations.

It turns out that extracting the thickness and refractive index from a measured "optical thickness" is not straightforward, particularly for layer thicknesses below 10 nm. One of the few methods is the use of an optical waveguide as substrate for the adsorbing protein. Here, the thin layer is probed by the evanescent field of a guided mode propagating through the waveguide structure. If the proportion of the evanescent field intensity within the thin layer relative to the overall intensity distribution in the waveguide structure can be varied, then thickness and refractive index of the thin layer can be determined. This has been demonstrated by varying the refractive index of the water solution [3], but this method is very tedious; in addition, the protein at the interface could change its properties depending on the composition of the bulk solution. A better approach is to exploit the different evanescent wave penetration depths associated with different guided modes that can exist within the waveguide structure.

In this paper, we describe a new method that allows for a separate determination of layer thickness and refractive index. Similar to the work in Lukosz' group [5], we will use the different polarization directions to obtain a controlled variation of the evanescent field's penetration depth. The method will be illustrated with the measurement of the real-time adsorption behaviour of a protein.

2. Determination of thickness and refractive index of an adsorbing layer

Consider a waveguide structure as depicted in Fig. 1. Proteins in the bulk solution interact with the surface of the waveguide, eventually forming an adsorbed monolayer. This process can be optically considered as the formation of a thin layer of thickness d_p and refractive index n_p.

* Corresponding author.

SSDI 0040-6090(95)08459-2

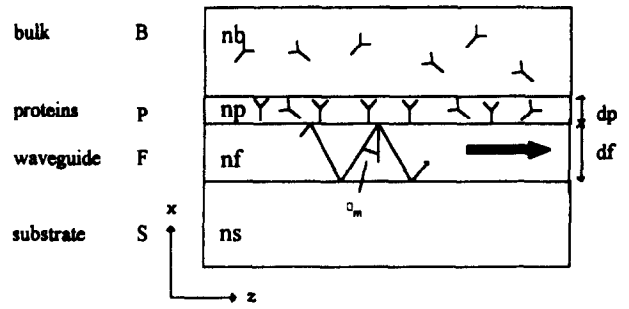

Fig. 1. Side-view of the planar waveguide structure. For explanation of symbols, see text.

It is well known (see, for example, Ref. [6]) that light propagation in a dielectric structure of Fig. 1 can be described by an "effective refractive index" N_{eff} of the waveguide, which is related to the propagation constant β_m of guided modes in the waveguide:

$$(N_{\text{eff}})_m \equiv \beta_m / k_0 = n_f \sin \theta_m \quad (1)$$

where k_0 is the propagation constant of the light in vacuum and n_f is the refractive index of the light guiding layer. The optical mode m is completely specified by the propagation angle θ_m, and thus $(N_{\text{eff}})_m$, and the polarization state (TE, TM) of the incident light. $(N_{\text{eff}})_m$ can be obtained by solving the mode equation (see Appendix) for the specific dielectric structure such as shown in Fig. 1, and the specified polarization state of the propagating mode.

The penetration depth of the evanescent field associated with each of these modes is different. Solving the mode equation for the situation of Fig. 1 for two values of m or for both polarization states, with known effective refractive indices and known waveguide material constants, results in two equations with two unknowns d_p and n_p. Combination of the expressions for the TE and TM propagation then provides the two required equations. In order to obtain maximum surface sensitivity the waveguide thickness d_f has to be chosen such that only one TE and only one TM mode propagate.

Contrary to previously published procedures, which are only valid for very thin layers [3,5] this approach provides exact expressions, which can be applied to layers of arbitrary thickness. An outline of these equations is given in the Appendix.

3. Principle of detection

We have developed a new method of measurement of N_{eff} that is based on the use of gradient effective index waveguides [7–9]. In a deflection sensor this gradient is created by an etched area in the cover layer (in this case, with a triangular shape, see Fig. 2). Only in this sensor area, a biochemical reaction (i.e. a protein adsorption), within the evanescent field of a propagating mode, changes the guiding properties of the waveguide (N_{eff}). According to Snell's law, this causes a change in deflection angle $\Delta\alpha$. This can be transformed into a translation by a lens, which can be detected with a CCD array.

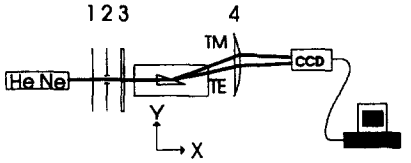

Fig. 2. Experimental set-up. In the triangular area protein adsorption is monitored by the evanescent fields of the TE and TM modes. (1) halfwave plate, (2) stop, (3) cylindrical lens $f=50$ mm, (4) lens $f=60$ mm. For more details, see text.

With an adequate choice of the geometry and material in the design of the deflection sensor a resolution of 1×10^{-5} in the measurement of N_{eff} is obtained. For a thickness $d_p = 0$ (2 nm) which is the situation we will deal with, this corresponds to a resolution of $\Delta n_p = 0.01$.

4. Experimental

The fabrication of the monomode waveguide chip has been described previously [9].

A schematic of the optical set-up used for the measurements is shown in Fig. 2. Light from a 2 mW He–Ne laser is end-coupled into a planar waveguide using a cylindrical lens. A half-wave plate is adjusted in such a way that both TE and TM modes are coupled into the waveguide with approximately the same intensity. By positioning the CCD array in the focal plane of the lens beam deflection is transformed into a translation. The position of the modes on the CCD array is recorded using a PC in which a video frame grabber (Videoblaster from Creative labs) was installed. A teflon cuvette ($\sim$0.5 ml content) is pressed to the waveguide structure with a silicon rubber seal in between.

Prior to an adsorption experiment, the sensor was calibrated by applying bulk refractive index steps. First the cuvette was filled with 0.4 ml of deionized water. Then 50 ml of the cuvette content was replaced by a glucose solution ($n \sim 1.36$). After stirring and a stabilization period of a few minutes, the positions of both TE and TM modes on the CCD

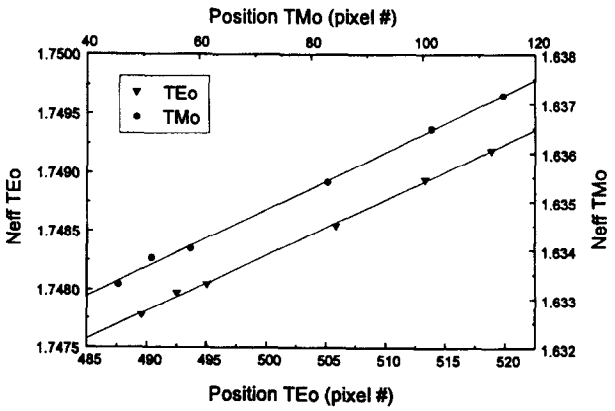

Fig. 3. Example of the result of a calibration procedure. The perfect linearity permits an N_{eff} determination better than 10^{-5}.

array were recorded. This procedure was repeated several times in 100 ml aliquots of the glucose solution. The refractive index of the solutions was determined with an Abbe refractometer. With these values, the effective refractive indices were calculated. A representative example of such a calibration is shown in Fig. 3. The slope of the experimentally determined line was used in the adsorption experiments to convert a pixel number into a value for N_{eff}.

Following the calibration the cuvette was washed by repeated substitution of half of the cuvette content by deionized water, until the angular positions of the TE and TM modes returned to their original values. Subsequently the cuvette was filled with buffer (PBS).

Polyclonal goat anti-human serum albumin (a-HSA, MW ~ 150 kD), and HSA (MW ~ 67 kD) were purchased from Sigma. Stock solutions of 6.7 mM and 0.67 mM were prepared in PBS (pH 7.3). Aliquots of these stock solutions were added to the 0.4 ml PBS solution in the cuvette to result in concentrations as indicated in Fig. 4 and Fig. 5.

5. Results and discussion

In Fig. 4 a representative example is shown of the results of an adsorption experiment with a-HSA (for details, see captions). Fig. 4(b) and 4(c) were obtained by processing

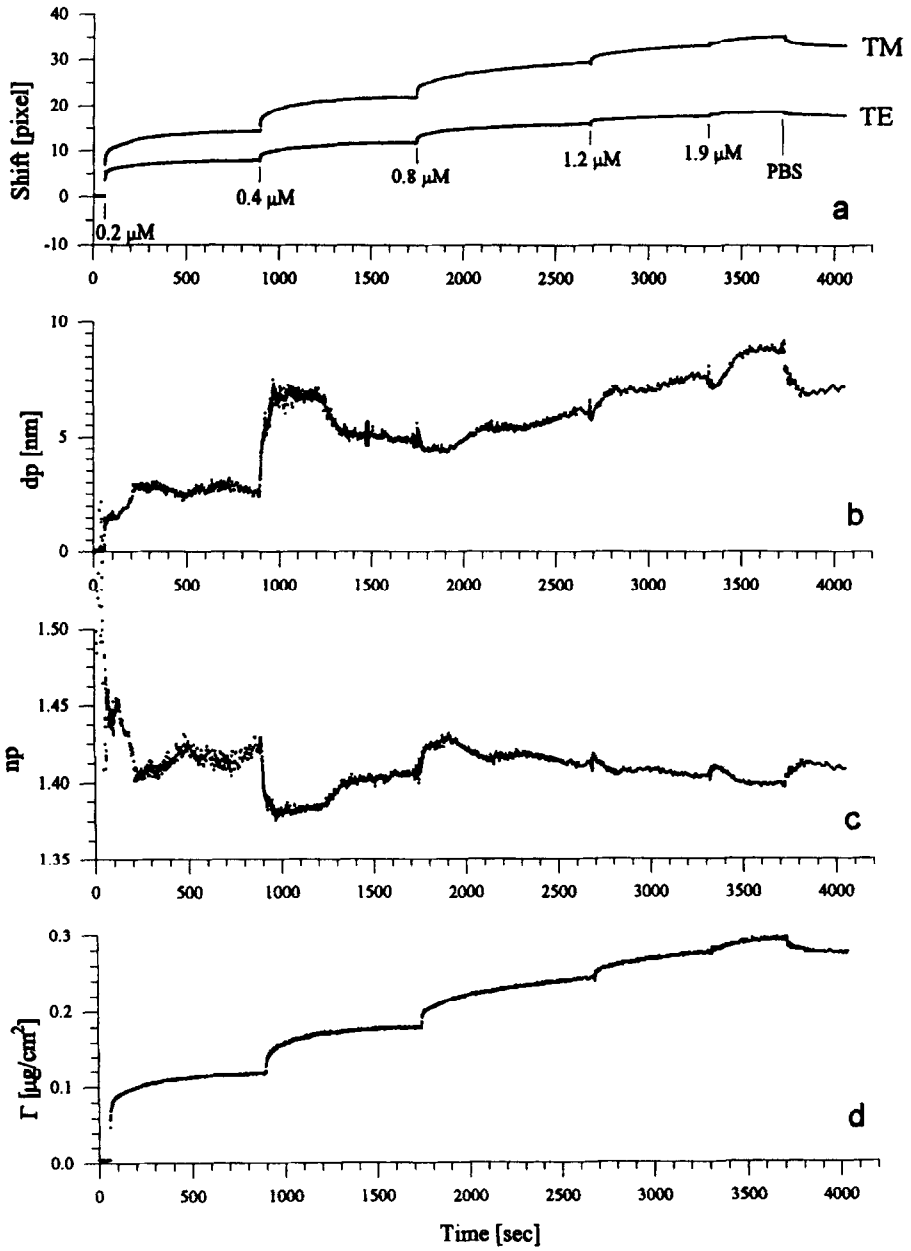

Fig. 4. Adsorption of a-HSA to Si_3N_4 substrate as a function of time. The adding of the various bulk protein concentrations in the course of time is indicated. At $t = 3500$ s the surface is rinsed with PBS. (a) raw data; (b), (c) d_p and n_p; (d) surface coverage (see Eq. (A5)). In (b) an error bar is indicated at $t = 1500$ s, corresponding to a systematic error of 0.2 pixel.

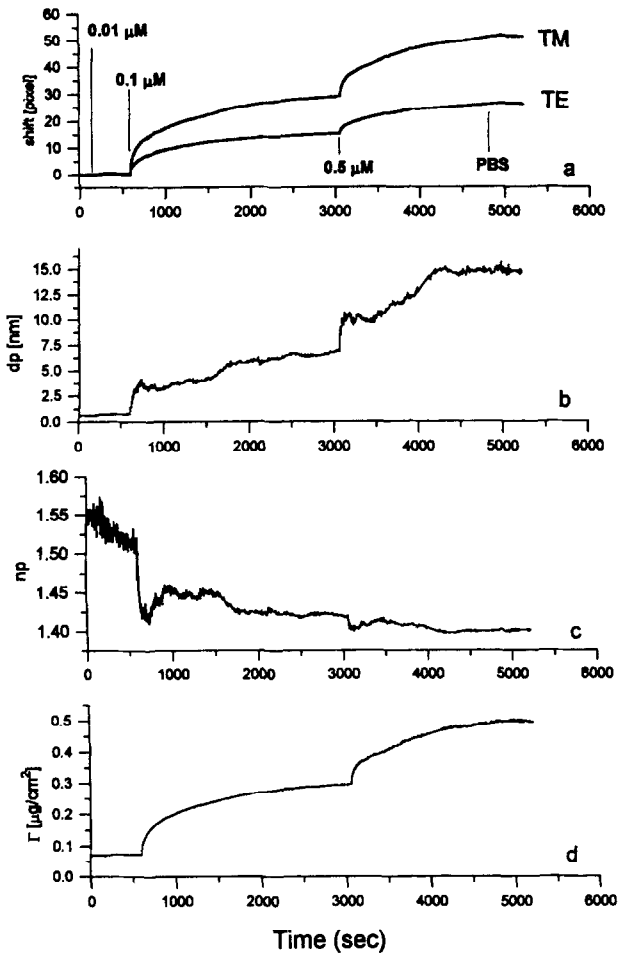

Fig. 5. Immunoreaction of a-HSA to HSA surface. For details, see caption to Fig. 4.

the experimental data of Fig. 4(a) according to the procedure mentioned in the Appendix.

It is seen that with smooth experimental data (Fig. 4(a)) the calculated thickness and refractive index sometimes show relatively abrupt changes. Because this type of variations is seen in most of our results, also on other proteins, one wonders of course whether this is due to instrumental or methodological shortcomings, and an error analysis of these data is necessary. The following tests were carried out.

1. In all cases solution of the equations mentioned in the Appendix resulted in one single pair of d_p, n_p values.
2. Only a temperature variation of the bulk solution by more than 5 °C has a significant effect on the calculated d_p, n_p. Also, systematic errors in the bulk refractive index only affect absolute values of d_p and n_p. This may be the reason that in some experiments we found small jumps in d_p, n_p when changing solutions (cf. Figs. 4 and 5).
3. The experimental uncertainty in the position of both emerging spots is 0.05 pixel. After adding an additional amount of noise of 0.1 pixel unit to the experimental data, we recalculated the d_p, n_p. Only the noise in the calculated data increased to approximately 0.01 refractive index unit and approx. 0.5 nm in the thickness; the overall form of the curves did not change.
4. A systematic error in the experimental data was simulated by adding angle-dependent pixel-offsets (maximum 0.2 pixels) to the raw data; the worst case was considered where the TM response was offset negatively, and the TE response was simultaneously offset positively. From the inset in Fig. 4 it can be concluded that this can have a significant effect on the form of the d_p, n_p curves. However, it should be mentioned that such a systematic shift of the measured data points is outside the noise range of 0.05 pixel units. In fact, in view of the calibration procedure utilized there cannot be a systematic error of this type; this calculation was only included to demonstrate what the effects are when within the noise band the measured curves are rotated.
5. It can be demonstrated that for a layer growth where n_p is constant the ratio between the TE-mode angular change and that of the TM mode does not change. In one set of calculations n_p was forced constant, and the ratio of TE change to TM change in the course of adsorption was calculated. The thus obtained calculated TE change was compared to the actually observed TE mode behaviour. It was found that the pixel position of these two modes could differ as much as 0.5 pixels, i.e. an order of magnitude larger than the experimental accuracy.

From these tests we conclude that the overall shapes of the d_p, n_p curves reflect aspects of the nature of the protein adsorbing at the surface.

In the following we will only discuss the main features of the adsorption events for a-HSA.

In Fig. 4 we see that at low bulk concentration d_p and n_p reach some steady-state value; by applying a higher concentration n_p goes down, and the average layer thickness grows. Then, after some time d_p, n_p change spontaneously and stepwise. The rest of the adsorption proceeds in a relatively smooth way, characterized by increasing d_p and decreasing n_p. Finally a plateau value is reached at $d_p \sim 10$ nm, consistent with the dimensions of an antibody. We want to stress that the spontaneous stepwise change is always observed when a bulk concentration around 0.5 mM of a-HSA is applied. It is also remarkable that this stepwise change is completely absent in Fig. 4(d) where the time course of the surface concentration is depicted.

In Fig. 5 are shown some representative results for the binding of a-HSA to a precoated HSA surface. At the onset of the experiment we see the high n_p of HSA, which we will not discuss here; after addition of a-HSA the refractive index of the whole layer decreases, indicating a-HSA binding. After addition of a higher concentration both d_p and n_p change. The overshoot observed particularly for n_p can hardly be attributed to some experimental artefact because this is also observed at addition of 0.5 mM a-HSA where the associated changes in pixel position are more than 20 units, i.e. far more than any experimental error.

Comparing Figs. 4 and 5 we observe that at the interface a-HSA as an adsorbing molecule behaves differently from that when involved in an immunoreaction: in the latter case

binding to the surface manifests itself mainly as an increase in average layer thickness. The fact that in Fig. 5 a plateau thickness is found of ~15 nm is consistent with the speculation that in the immunoreaction a-HSA binds with its long axis perpendicular to the substrate.

6. Conclusion

We have demonstrated that refractive index and average layer thickness of a thin layer can be separately determined using a very simple planar waveguide structure. The found end values for d_p are in line with known dimensions of the a-HSA molecule [10].

Beyond doubt, our experimental data point to conformational and/or orientational changes of the protein while interacting with the surface. However, a more detailed discussion requires an optical model on the interpretation of n_p in the case of submonolayer coverage. The main difficulty here is how light interacts with a non-homogeneous thin layer. Possibly, the work of Raether [11] on surface plasmon resonance of rough surfaces can be adapted to this problem. Furthermore, we want to note that the used model is formally only applicable to optically isotropic systems. Although we do no not expect that this is a serious limitation for the globular systems considered here, this point also deserves further study.

Appendix A

We consider a four-layer structure (Fig. 1); the light undergoes total internal reflection at the substrate S and at the cover, which consist of two layers (i.e. a protein layer P and a buffer solution B). The dispersion relation is [6]:

$$\Phi_{tot} = 2k_{x,f}d_f + \Phi_{f,s} + \Phi_{f,p,b} = 2\pi m \quad m = 0, 1, 2 \ldots \qquad (A1)$$

where $k_{x,f} = k_0(n_f^2 - N_{eff}^2)^{1/2}$, $k_0 = 2\pi/\lambda_0$ (λ_0 is the wavelength in vacuum) and m is the mode number. $F_{f,s}$ and $F_{f,p,b}$ are the phase shifts as a result of total internal reflection at the interface F/S and at the F/P/B structure respectively.

The phase shift $F_{f,j}$ can be calculated with the Fresnel reflection coefficient $r_{f,j}$ at the interface F/J by $r_{f,j} = \exp(iF_{f,j})$. For the phase shift $F_{f,p,b}$ built up after reflection at a two-layer structure (reflection coefficient $r_{f,p,b}$) the following expression is found:

$$\Phi_{f,p,b} = 2\arctan\left[i\frac{(1-r_{f,p,b})}{(1+r_{f,p,b})}\right]$$

$$= 2\arctan\left[i\frac{1-r_{f,p}}{1+r_{f,p}}\frac{1-r_{p,b}\exp(2ik_{x,p}d_p)}{1+r_{p,b}\exp(2ik_{x,p}d_p)}\right] \qquad (A2)$$

where $k_{x,p} = ik_0(N_{eff}^2 - n_p^2)^{1/2}$ is the imaginary propagation constant of the associated mode. Analytical expressions for $r_{i,j}$, the reflection coefficient for reflection at the interface I/J, can be found in Ref. [6].

For the zero order modes ($m = 0$) we derive, using Eqs. (A1) and (A2):

$$d_p = \frac{-1}{2|k_{x,p}|}\ln\left[\frac{1}{r_{p,b}}\frac{1-Z}{1+Z}\right] \qquad (A3)$$

where

$$Z = \frac{k_{x,f}}{|k_{x,p}|}\left(\frac{n_p}{n_f}\right)^{2p}\tan\left[k_{x,f}d_f + \frac{\Phi_{f,s}}{2}\right] \qquad (A4)$$

where r is a polarization factor ($r = 0$ for TE and $r = 1$ for TM modes). The variables $k_{x,f}$, $k_{x,p}$, $r_{p,b}$ and $F_{f,s}$ change with the effective refractive index N_{eff}.

A measurement of N_{eff} of the two different polarization states will provide the two equations from which d_p and n_p can be calculated.

The surface coverage Γ can be calculated from [2]:

$$\Gamma = d_p(n_p - n_b)/\delta \qquad (A5)$$

with $\delta = 0.188$ ml g^{-1} the refractive index increment of a protein as function of the concentration.

References

[1] H. Arwin and D.E. Aspnes, *Thin Solid Films, 113* (1984) 101.

[2] J.A. de Feyter, J. Benjamins and F.A. Veer, *Biopolymers, 17* (1978) 1759–1772.

[3] H.E. de Bruijn, B.S.F. Altenburg, R.P.H. Kooyman and J. Greve, *Opt. Commun., 82* (1991) 425–432.

[4] R.P.H. Kooyman, H.E. de Bruijn, R.G. Eenink and J. Greve, *J. Mol. Struct., 218* (1990) 345–350.

[5] K. Tiefenthaler and W. Lukosz, *J. Opt. Soc. Am. B, 6* (1989) 209–220.

[6] H. Kogelnik, Theory of dielectric waveguides, in T. Tamir (ed.), *Topics in Applied Physics*, Vol. 7: Integrated Optics, Springer–Verlag, Berlin, 1975.

[7] R.E. Kunz, *Sensors Actuators., B11* (1993) 167–176.

[8] R.G. Heideman, Optical waveguide based evanescent field immunosensors, *Thesis*, University of Twente, 1993.

[9] E.F. Schipper, R.P.H. Kooyman and J. Greve, *Sensors Actuators, B24* (1995) 90–93.

[10] D.R. Davies and E.A. Padlan, *Ann. Rev. Biochem., 59* (1990) 439–473.

[11] H. Raether, *Surface Plasmons*, Springer Tracts in Modern Physics, Vol. 111, 1988, Springer, Berlin.